Analysis of a methane partial oxidation mechanism relevant at the conditions of the anode channels of a solid-oxide fuel cell

Á. Kramarics, I. Gy. Zsély, T. Turányi*

Institute of Chemistry, Eötvös University (ELTE), Budapest, Hungary
H-1117 Budapest P.O. Box 32.

Abstract

Solid-oxide fuel cells can efficiently generate electric power. One of their great advantages is that they can be operated with hydrocarbon fuels. Composition of the fuel mixture in the anode channel greatly affects the performance of the fuel cell. A detailed reaction mechanism of 350 species and 6874 irreversible reactions has been created by Dean *et al.* to describe the homogeneous gas-phase chemistry in the anode channel. This mechanism, due to its large size, cannot be used directly for industrial optimalization. A reduced mechanism of 168 species and 1834 reactions was derived, which provides simulation results 7 times faster, while the results agree within a few percent.

Introduction

Fuel cell technology is one of the most promising opportunities for generating energy with decreased environmental impact. In the last decades several types of fuel cells have been developed. Scientists keep changing their minds every few years about which types of the fuel cells will be the most popular in the future. One of the great advantages of solid-oxide fuel cells is their absolute tolerance to CO, unlike the other types of fuel cells *e.g.* SPEFCs (solid polymer electrolyte fuel cells). Furthermore, in solid-oxide fuel cells several available fossil fuels can be used, thus there is no need to build a hydrogen delivery infrastructure [1]. In hybrid systems, where a gas turbine is built in the SOFC, the efficiency can reach 75-80 % [2].

The core of the SOFC is a solid electrolyte, which is a conductor for oxide-ions at the operating temperature. In practice, yttria stabilized zirconium-dioxide is used for electrolyte. During the operation of the solid-oxide fuel cell, oxygen is reduced at the cathode, the formed oxygen anion then diffuses across the oxide-ion selective electrolyte, which is electrically insulating. Although solid-oxide fuel cells have so far been operated with methane, propane, butane, fermentation gas, gasified biomass and paint fumes [3], the hydrocarbon fuel is first converted to CO and H_2 by steam reforming, either within the anode region or externally. In the three-phase region, hydrogen is electrochemically oxidized by the oxygen anions to form water and electrons. This water then participates in the water gas shift reaction to convert CO to CO_2 and H_2, and this H_2 is subsequently oxidized in the three-phase region.

In a solid-oxide fuel cell, chemical reactions take part at three places: in the anode channel (homogeneous gas-phase kinetics), on the surface of the porous anode (heterogeneous catalysis) and at the three-phase boundary between the anode and the electrolyte (electrochemical catalysis). Homogeneous chemical reactions can change the composition of the initial fuel; therefore, modify the species that will undergo electrochemical oxidation.

Solid-oxide fuel cells can operate with hydrocarbon fuels and the inlet fuel mixture flows through a heat exchanger. The operating temperature is about 800–1000 °C and therefore the homogeneous gas-phase reactions are significant before the fuel mixture reaches the anode. If a pure hydrocarbon gas enters the anode channel, at these temperatures the fuel starts to pyrolyze. The hydrocarbon forms mostly smaller species (alkanes, olefins, and H_2), but there is also the potential for molecular weight growth to occur that might lead to deposit formation.

These species are the indicators of a propensity to form carbonaceous deposits [4]. The oxidative pyrolytic reactions convert the initial hydrocarbons to H_2, CO, H_2O and other products, and may also lead to the formation of polyaromatic hydrocarbon deposits. These deposits can damage the porous structure of the anode, and can abridge the life of the cell. Deposit formation can be related to the concentration of species having more than four carbon atoms, denoted by C^{5+} [5]. Deposit formation is a function of the residence time and the initial composition of the mixture. Air and water steam may be added to the initial fuel to prevent deposit formation. In our calculations we assume that the fuel is free from impurities (*e.g.* sulphur).

Anthony Dean and his group study the homogeneous gas-phase anode channel reactions of solid-oxide fuel cells. Recently, a detailed reaction mechanism was created and tested [5] that is applicable at solid-oxide fuel cell operating conditions. It can model the reactions of methane and natural gas, with air and/or steam added. In this study, a further developed (2006 May) version of this mechanism was investigated.

Simulations with the original mechanism

The initial reaction mechanism includes 348 reactive species and species N_2 and Ar. At the conditions of the anode channel of a solid-oxide fuel cell, N_2 and Ar do not participate in chemical reactions, but their

* Corresponding author: turanyi@chem.elte.hu

concentration affect the concentration of other species through third-body reactions. The reactive species consist of C, O and H elements. The initial mechanism includes 3456 reversible reactions. These reactions were transformed to irreversible ones by program MECHMOD [6]. The obtained mechanism contains 6874 irreversible reactions.

The CHEMKIN 4 program package [7] was used for the simulations. The operating conditions of a solid-oxide fuel cell can vary across a wide range of conditions, and we selected initial parameters that generally represent well the SOFCs. Thus, temperature and pressure were chosen to be 900 °C (1173.15K) and 1 atm (101325 Pa), respectively. The simulations were carried out at isothermal and isobaric conditions. The composition of the initial mixture was 30.0 % v/v methane and 70.0 % v/v air. The assumed composition of air was 79 % v/v nitrogen and 21 % v/v oxygen. Unfortunately, the homogeneous kinetics solver of CHEMKIN 4 provides the concentrations only in equal time intervals; therefore to cover the logarithmic time-scale, three simulations were carried out. In the first case, the total time was 1 s, with time step of 0.01 s, in the second case the total time was 100 s with time step of 1 s, and in the third case the total time was 1000 s with time step of 10 s. The simulation results can be seen in Figure 1.

The mole fraction reaches or exceeds $x = 0.001$ for the following species: CH_4, O_2, N_2, CO, CO_2, H_2CO, H_2, H_2O, C_2H_6, C_2H_4, C_2H_2 and benzene (C_6H_6). It is clear that the mixture burns out in about 1 s. During this time, the mole fraction of oxygen is reduced from its initial value ($x(O_2) = 0.147$) to $x(O_2) = 0.0042$. After 1 s, the mole fraction of methane decreases in a slower rate. It is interesting to inspect the mole fraction–time curves of the main products, CO, CO_2, H_2 and H_2O. In the initial period of the reaction (till about 1 s), the mole fractions of these species monotonically increase. After 5 s, this behaviour changes; the mole fractions of CO and H_2O decrease, while the mole fractions of CO_2 and H_2 increase. This is the gas-phase equivalent of the catalytic water gas shift reaction. The profiles of the mole fractions of C_2H_6, C_2H_4 and C_2H_2 have a characteristic shape. Each curve has a maximum; in the mole fraction–time curve of C_2H_6 and C_2H_4 this maximum is very sharp, while in the mole fraction–time curve of C_2H_2 the peak is blunt. The most interesting is the shifted locations of these maximums. The mole fraction maximums of C_2H_6, C_2H_4, and C_2H_2 appear at 0.11 s, 0.43 s, and 26 s, respectively. In the initial period of the reaction, the mole fraction of benzene increases very significantly ($x(C_6H_6) = 9.96 \cdot 10^{-10}$ at 0.1 s and $x(C_6H_6) = 3.49 \cdot 10^{-6}$ at 1 s). After 1 s, this rising slows down ($x(C_6H_6) = 9.98 \cdot 10^{-5}$, $9.83 \cdot 10^{-4}$, and $2.92 \cdot 10^{-3}$ at 10 s, 100 s, and 1000 s, respectively).

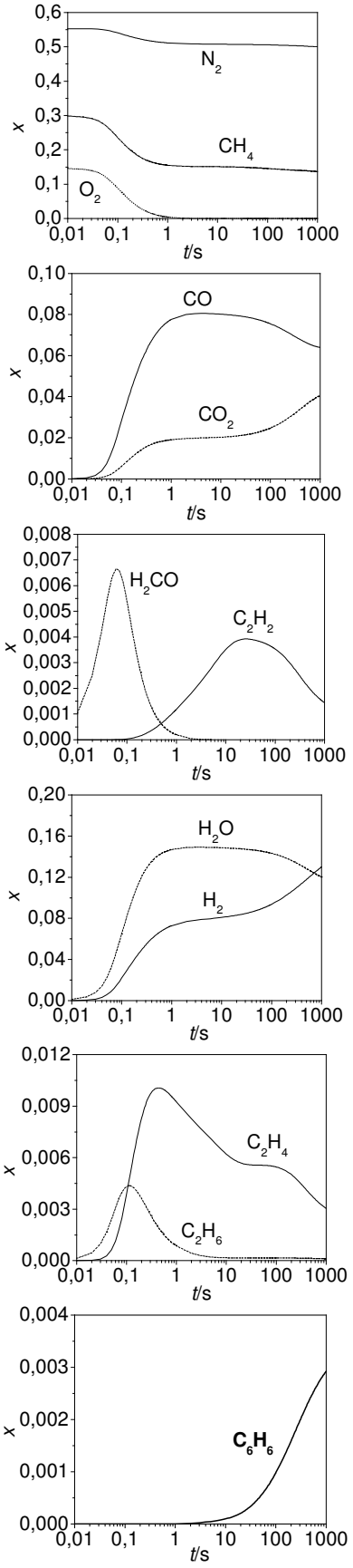

Figure 1. Mole fraction–time profiles in a methane–air mixture ($x(CH_4)_{initial} = 0.3$, $T = 900$ °C, $p = 1$ atm)

Mechanism reduction

The Dean mechanism is too large for industrial optimalization work and therefore reduction is needed. Our purpose was to find a reduced mechanism, which contains less species and fewer reactions, but its simulation reproduces the results obtained using the original mechanism within a few percent.

The reduction was carried out in two steps: first the redundant species, then the redundant reactions were eliminated. A possible algorithm for the detection of redundant species can be based on the inspection of the normalized Jacobian $\tilde{\mathbf{J}}_{ij} = (y_i / f_j)(\partial f_j / \partial y_i)$. An element of the normalized Jacobian provides information about how the production rate of species j changes, if the concentration of species i is perturbed. If the square of changes is summed up for all important species, then the obtained value B_i characterizes the strength of the direct link of species i to the group of important species: $B_i = \sum_{j=1} ((y_i / f_j)(\partial f_j / \partial y_i))^2$

Species having high B_i values are closely linked to the important species. In the next step, the species having the highest B_i value is also included into the summation and vector **B** is recalculated. This procedure is repeated until a gap appears in the series of the ordered B_i values. Species having B_i values above the gap are closely linked directly or through other species to the important species; these are the necessary species. Because the Jacobian depends on the concentrations, the redundancy of species has to be investigated at several reaction times. A species is redundant, if it is redundant at each time investigated. All consuming reactions of the redundant species can be eliminated from the mechanism. More details about the detection of redundant species are discussed in [8] and [9]. This algorithm is encoded as option CONNECT in KINALC [6].

In simpler cases, redundant species can be easily identified with the method above. In the cases of larger mechanisms this gap does not appear. So we had to modify our method: at each observed reaction time the first 80 species were added to the important species, and after this the sets were combined. This way, the necessary species were identified.

Important species were those species, for which the maximum of mole fraction is higher than 0.001. The analysis was carried out at the following 11 reaction times: t = 0.01 s, 0.03 s, 0.1 s, 0.3 s, … , 1000 s; these times are positioned evenly on a logarithmical time scale. Necessary species were identified at each reaction time. All in all, 182 species were proved to be redundant, so the species-reduced mechanism contains only 168 species. Elimination of the reactions of the redundant species resulted in a 3027 irreversible step mechanism. To check how the results of the original and the reduced mechanisms differ from each other, we made three simulations using the same final reaction times and time steps as before. Good agreement of the mole fractions of the important species was found, when the mole fractions were higher then 0.001. Accordingly, good agreement was found for the mole fractions of CH_4, N_2, CO, CO_2, H_2, H_2O, C_2H_4 and C_2H_2 during the whole time-interval; O_2, H_2CO and C_2H_6 till 1 s; and benzene (C_6H_6) from 100 s. The largest difference was 7.11 %, which was found for the mole fraction of C_2H_2 at t = 0.11 s. At this time the mole fraction of C_2H_2 is very low ($x = 4.12 \cdot 10^{-5}$), but it is higher than one percent of the mole fraction maximum (x_{max} = 0.00393).

In the next step, redundant reactions were eliminated. A possible method for the elimination of redundant reactions from detailed reaction mechanisms is the principal component analysis of the rate sensitivity matrix **F** (PCAF method) [10]. Eigenvector–eigenvalue analysis of matrix $\tilde{\mathbf{F}}^T\tilde{\mathbf{F}}$ provides the list of important reactions, where in matrix $\tilde{\mathbf{F}} = \{(k_j / f_i)(\partial f_i / \partial k_j)\}$ index i refers to the important and necessary species, and j refers to all reactions of these species. All important reactions have large eigenvector elements in a parameter group characterized by a large eigenvalue. A reaction is redundant, if it is found to be redundant at each time investigated.

Using option PCAF of KINALC [6], redundant reaction steps were eliminated. The importance of reactions was observed at the same 11 reaction times, and the thresholds for eigenvalues and eigenvectors were 10^{-8} and 10^{-8}, respectively. Considering all reaction times, 1193 irreversible reactions were found to be redundant. So, the reduced mechanism contains only 1834 irreversible reactions of 168 species. We observed good agreement of the mole fractions of the important species, when their mole fraction was higher then 0.001. Thus, good agreement was observed for species CH_4, N_2, CO, CO_2, H_2, H_2O, C_2H_4 and C_2H_2 during the whole time-scale; O_2, H_2CO and C_2H_6 till 1 s, and benzene (C_6H_6) from 100 s. The largest difference was 6.90 % for the mole fraction of benzene at t = 970 s. The comparison of the results obtained using the original and the reduced mechanisms can be seen in Figure 2.

The simulation times required for the original full and the final reduced mechanisms were compared and the latter was found to be 7 times less. It means that this mechanism reduction can be a significant step towards the industrial application of the reaction mechanism for the anode channel kinetics.

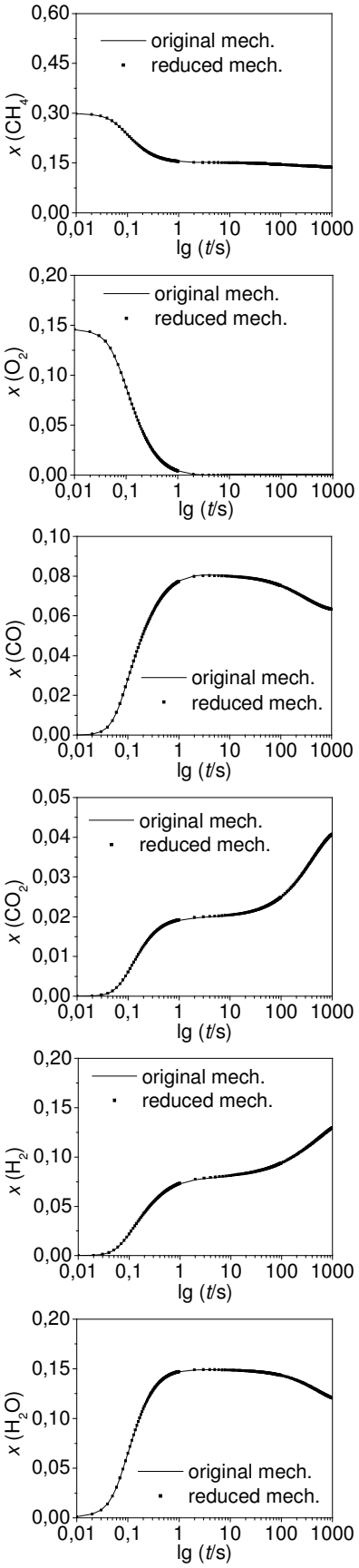

Figure2. Comparison of the results obtained by the original (line) and the reduced (dots) mechanisms.

Effect of changing the composition of the initial mixture

The effect of the various initial compositions was investigated in two series of simulations using the original mechanism. During these simulations, pressure and temperature were kept at constant 1 atm and 900 °C, respectively. In both series of simulations, the initial mole fraction of methane was x = 0.3. Results are illustrated on a series of contour plots showing mole fractions of species as a function of residence time (x axis) and the initial mole fraction of steam (y axis).

In the first series of simulations, the initial mixture consisted of methane, air and steam. Mole fraction of steam was varied from 0.7 to 0. Accordingly, the initial mole fraction of air changed from 0 to 0.7. Results are given in Figure 3.

It is clear from Figure 3 that the time history of each concentration depends very much on the initial composition. In air rich mixtures, the decrease of the mole fractions of methane and oxygen are fast between 0.1 s and 0.3 s. In these mixtures, the mole fraction–time curves of carbon monoxide have a maximum. The rise of the mole fractions of carbon dioxide and hydrogen is very steep between 100 s and 1000 s and between 30 s and 300 s, respectively. The rate of decrease of the mole fractions of methane and oxygen is smaller in steam rich mixtures, and the amount of carbon dioxide produced is much less than in air rich mixtures.

In the second series of simulations, the initial mixture consisted of methane, steam and CO_2. Mole fraction of steam was varied from 0.7 to 0, and thus the initial mole fraction of CO_2 changed from 0 to 0.7. Results are given in Figure 4.

Comparing with the previous figure, in Figure 4 the concentration changes are much slower, and there is less dependence on the initial composition. There are almost vertical gridlines on some of the contour plots (methane, hydrogen). Until about 30 s, there is no change in the mole fractions of the components of the initial mixture. The mole fraction curves of carbon monoxide and hydrogen are monotonically increasing. In water rich mixtures the mole fraction of the formed hydrogen is higher, and the mole fraction of water decreases. In carbon dioxide rich mixtures the mole fraction of carbon monoxide is higher, the consumption of methane and carbon dioxide is faster, and the mole fraction of water increases with time. These mixtures initially did not contain oxygen, therefore the mole fraction of oxygen is always very small, but there is a maximum on the mole fraction – time curve at about 30s.

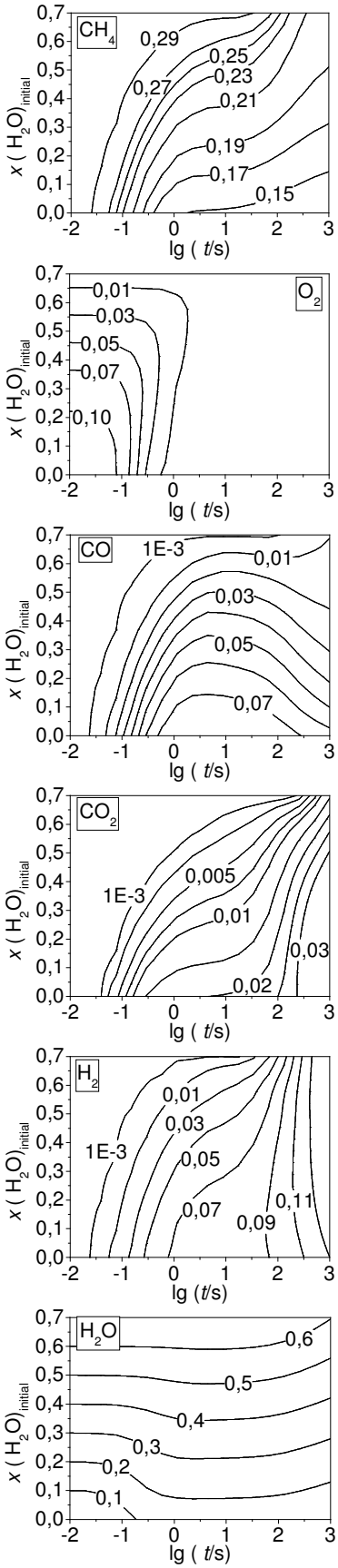

Figure 3. Mole fractions in a methane – air – steam mixture as a function of time and the initial mole fraction of steam ($x(CH_4)_{initial}$ = 0.3, T = 900 °C, p = 1 atm)

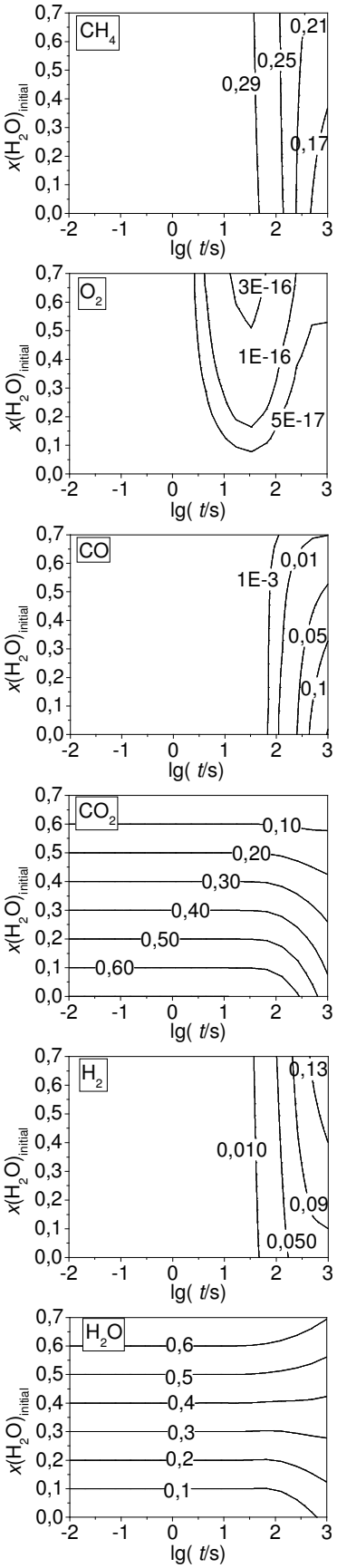

Figure 4. Mole fractions in a methane – carbon dioxide – steam mixture as a function of time and the initial mole fraction of steam ($x(CH_4)_{initial}$ = 0.3, T = 900 °C, p = 1 atm)

Conclusions

Solid-oxide fuel cells (SOFCs) are very promising energy sources. Development of more efficient SOFCs can be based on computer aided design (CAD) codes. These CAD codes have to take into account the chemical reactions that take part in the anode channel (homogeneous gas-phase kinetics), on the surface of the porous anode (heterogeneous catalysis) and at the boundary between the anode and the electrolyte (electrochemical catalysis). Recently, a detailed reaction mechanism of 350 species and 6874 irreversible reactions was proposed by Dean *et al.* [5] to describe the homogeneous gas-phase chemistry in the anode channel.

Our first aim was to find a reduced mechanism that is much smaller, but is able to reproduce the results of the original mechanism within a few percent. The obtained reduced mechanism contains 168 species (less, than half of the number of species in the original mechanism) and 1834 irreversible reactions (which is 5000 reaction steps less). The simulation time needed is 7 times less using this reduced mechanism.

The effect of changing the composition of the initial mixture was also studied. It is clear that the presence of oxygen makes the reaction much faster. In air rich mixtures the decay of mole fractions of oxygen and methane and also the formation of carbon monoxide, carbon dioxide and hydrogen are fast. In methane – air – steam mixtures there are significant differences in the behaviour of air rich and steam rich mixtures. In methane – steam – carbon dioxide mixtures the changes are much slower and the dependence on the initial composition is less.

Acknowledgements

The authors are grateful for the support of OTKA grant T043770 and for Professor Anthony M. Dean and Dr. Hans-Heinrich Carstensen for providing their methane pyrolysis mechanism and the discussions.

References

[1] Ch. Y. Sheng, A. M. Dean, J. Phys. Chem. *A* 108 (2004) 3772-3783
[2] J. Brouwer, Fuel Cell Catalyst 1 (2000) 1
[3] http://en.wikipedia.org/wiki/Solid-oxide_fuel_cells
[4] K. M. Walters, A. M. Dean, H. Zhu, R. J. Kee, Journal of Power Sources 123 (2003) 182-189.
[5] G. Gupta, E. S. Hecht, H. Zhu, A. M. Dean, R. J. Kee, Journal of Power Sources 156 (2006) 434-447.
[6] http://garfield.chem.elte.hu/Combustion/Combustion.html
[7] http://www.reactiondesign.com
[8] T. Turányi, New J. Chem. 14 (1990) 795.
[9] I. Gy. Zsély, T.Turányi, PCCP 5 (2003) 3622
[10] T. Turányi, T. Bérces, S. Vajda, Int. J. Chem. Kinet., 21 (1989) 83.